

Spin-orbit splitting for single-particle and single-hole energies: Interplay of relativity and core polarization

L. Zamick

Department of Physics and Astronomy, Rutgers University, Piscataway, New Jersey 08855

D. C. Zheng

Department of Physics and Astronomy, McMaster University, Hamilton, Ontario, Canada L8S 4M1

H. Mütter

Institut für Theoretische Physik der Universität Tübingen, D-7400 Tübingen, Germany

(Received 21 January 1992)

The effects of core polarization on the single-particle energies and single-hole energies relative to a closed major shell core are considered. Not only the familiar two-particle–one-hole and three-particle–two-hole diagrams but also Hartree-Fock insertions are included. We further consider the effects of the Dirac spinor approach for nucleons inside the nucleus with a Dirac effective mass less than the bare mass and also for nucleons at the surface with an effective mass essentially equal to the bare mass. This relativistic effect tends to reduce the spin-orbit splitting of particle states as compared to that for hole states, which corresponds to the empirical data. The calculations are performed employing modern versions of the Bonn one-boson-exchange potentials with various strengths for the tensor component.

PACS number(s): 21.60.Cs, 21.60.Jz

I. INTRODUCTION

The motivation of this work is a better understanding of single-particle and single-hole energies in nuclei. In particular we would like to study the differences in the spin-orbit splittings of single-particle states above the Fermi energy and of single-hole states below the Fermi energy. In order to demonstrate that there are effects in these energy splittings which may require a microscopic analysis, we recall the experimental fact that the $p_{3/2}^{-1}p_{1/2}^{-1}$ single-hole splitting in ^{15}O is larger than the $d_{3/2}$ - $d_{5/2}$ single-particle splitting in ^{17}O . Provided one identifies the first $\frac{3}{2}^{-}$ level in ^{15}O as a single-hole state $[(p_{3/2})^{-1}]$ and the first $\frac{3}{2}^{+}$ level in ^{17}O as a single-particle state $[(d_{3/2})^1]$, the corresponding numbers are 6.176 and 5.086 MeV, respectively. But we know that for a one-body spin-orbit interaction of the form $-\xi l \cdot s$ with ξ taken to be a constant, the splitting between the spin-orbit partners $j=l-\frac{1}{2}$ and $j=l+\frac{1}{2}$ is proportional to $(2l+1)$. Hence the $d_{3/2}$ - $d_{5/2}$ splitting should be $\frac{5}{3}$ times the $p_{1/2}$ - $p_{3/2}$ splitting.

This problem persists in more sophisticated Skyrme Hartree-Fock (HF) calculations [1]. In a HF calculation for ^{16}O with the Skyrme III interaction, the $p_{1/2}$ - $p_{3/2}$ splitting turns out to be 6.0 MeV for neutrons and 5.9 MeV for protons, more or less in agreement with experiment; however, the $d_{3/2}$ - $d_{5/2}$ splitting is 7.8 MeV for neutrons and 7.4 MeV for protons, roughly in agreement with the $(2l+1)$ rule and thus in disagreement with the ^{17}O spectrum.

Since the spin-orbit term in the single-particle potential has basically a relativistic origin, it sounds quite plausible that nonrelativistic calculations, like the Skyrme Hartree-Fock calculations mentioned above, miss the rel-

ativistic degrees of freedom, which are needed to understand details in the spin-orbit splitting of single-particle levels. Recently we had found that the Dirac-Brueckner-Hartree-Fock (DBHF) approach to nuclear structure can lead to significantly different results from a nonrelativistic calculation [2]. The main feature of the DBHF approach is that the Dirac spinors for the nucleons inside a nuclear medium, characterized by the Dirac effective mass m^* , can be quite different from the Dirac spinors for nucleons in the vacuum, i.e., the effective mass m^* inside the nucleus is considerably smaller than the mass m of a free nucleon.

We considered, for example, the magnetic dipole ($M1$) excitation from the ground state to the lowest $J^\pi=1^+$, $T=1$ state in ^{12}C at 15.11 MeV. The experimental value of $B(M1)$ for this transition is $2.85\mu_N^2$. In a nonrelativistic approach with a bare Bonn A interaction [3], the value of $B(M1)$ was $0.64\mu_N^2$, much smaller than the experimental value. In the Dirac spinor approach with different effective nucleon masses m^* , the values of $B(M1)$ were calculated to be $0.69\mu_N^2$ for $m^*/m=1$, $1.14\mu_N^2$ for $m^*/m=0.78$, and $1.57\mu_N^2$ for $m^*/m=0.67$ [2]. The improved results were traced to the fact that the spin-orbit interaction in the Dirac spinor approach is nearly inversely proportional to m^* . Indeed, without core polarization, the $p_{3/2}^{-1}p_{1/2}^{-1}$ splittings relative to the ^{16}O for the above three (m^*/m) values are 3.95, 5.24, and 6.16 MeV, respectively.

Now in ^{12}C when the spin-orbit splitting is taken to be small one approaches the LS limit. In this limit the spin part of the $M1$ excitation vanishes so one is left with the orbital part. The orbital part is very small because it is proportional to the squared isovector g_l factor: $(g_l^V)^2 = \{[g_l(p) - g_l(n)]/2\}^2 = 0.5^2$, which is only about 1% of the squared isovector g_s factor:

$(g_s^V)^2 = \{[g_s(p) - g_s(n)]/2\}^2 = 4.706^2$. In the jj limit, on the other hand, the value of $B(M1)$ is $11.26\mu_N^2$, very large. Therefore one can obtain better agreement of the $B(M1)$ value with experiment by increasing the spin-orbit splitting as it is obtained from the DBHF approach.

For a comparison with experimental data it may not be sufficient to evaluate the single-particle energies in the Hartree-Fock or DBHF approximation. In particular for states close to the Fermi level, it might be necessary to account for the coupling of single-particle states to two-particle–one-hole (2p-1h) and three-particle–two-hole (3p-2h) configurations at low energies. This means that the inclusion of rearrangement terms or core polarization effects could be very important. Therefore it is the subject of this work to study the interplay between relativistic effects and core polarization terms in calculating single-particle energies and spin-orbit splittings.

As an example we study the effects for the nucleus ^{16}O for which the experimental data have already been discussed above. For the nucleon-nucleon (NN) interaction we consider the G matrix calculated for various modern versions of the Bonn one-boson-exchange (OBE) potentials [4]. It should be remarked at the outset that a double partitioning method is used to calculate the G -matrix elements of the Bonn interactions. Since we want to see explicitly the effects of the low-lying ladder excitations (up to $2\hbar\omega$), these low-lying ladders have been *excluded* from the G -matrix calculation. Thus there is no double counting in the calculations we perform.

II. RENORMALIZATION OF SINGLE-PARTICLE AND SINGLE-HOLE ENERGIES

In Fig. 1 we list all the first- and second-order diagrams to be included for the renormalization of the single-particle energies. Figure 1(a) represents the interaction of a particle in the orbit (nlj) (also denoted by j) with a particle in the core orbit c . The expression for this diagram, in the lowest order, including the kinetic energy obtained from a harmonic oscillator single-particle well, is as follows:

$$\begin{aligned} \epsilon_j(M) &= \epsilon_j(K) + \epsilon_j(V) \\ &= \left[2n + l + \frac{3}{2} \right] \frac{\hbar\omega}{2} \\ &\quad + \frac{1}{2(2j+1)} \sum_{c,J,T} (2J+1)(2T+1) \langle jc|V|jc \rangle_{J,T}, \end{aligned} \quad (1)$$

where the first term is the kinetic energy (n starts from 0) and the second the bare mean field interaction term. In the summation, c runs over all the orbits inside the core.

The value of $\hbar\omega$ and the particle-particle matrix elements $\langle jc|V|jc \rangle_{J,T}$ that we use in this work are those appropriate for nuclei around $A = 16$. It should be emphasized that all the expressions in this work are in terms of antisymmetrized and *unnormalized* particle-particle matrix elements.

In Fig. 1(b) we show a second-order core polarization

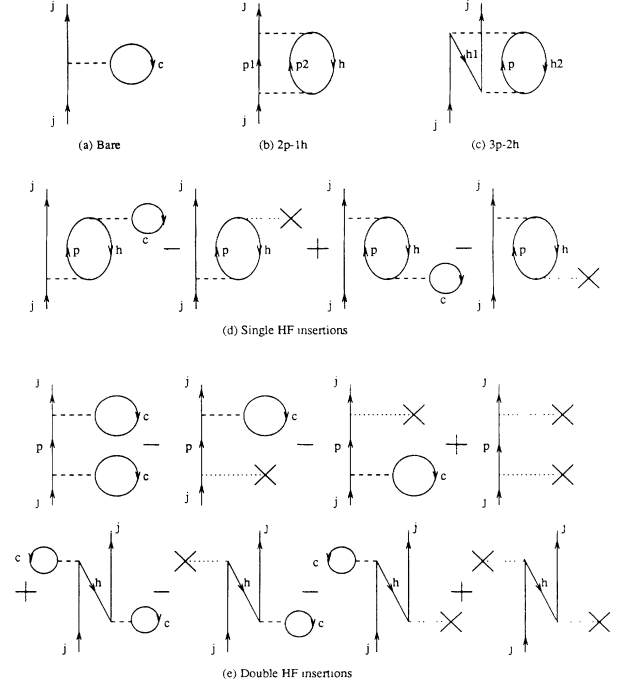


FIG. 1. The first- and second-order diagrams for single-particle energies. Dashed lines represent the particle-particle interaction V and dotted lines represent the one-body harmonic oscillator potential U .

diagram with a 2p-1h intermediate state. Its contribution to the single-particle energy can be written as

$$\begin{aligned} \delta\epsilon_j(2p-1h) &= \frac{1}{4(2j+1)} \sum_{h,p_1,p_2,J,T} (2J+1)(2T+1) \\ &\quad \times \frac{[\langle p_1 p_2 | V | j h \rangle_{J,T}]^2}{\epsilon_j + \epsilon_h - \epsilon_{p_1} - \epsilon_{p_2}}, \end{aligned} \quad (2)$$

where the sum over p_1, p_2 is an unrestricted sum over particle states. The above expression yields an attractive contribution for j denoting a hole state or a low-lying particle state, as we will do in our investigations, since the energy denominator is always negative for those states. From the energy denominator, one can also see that there is a tendency for this term to yield more attraction for states j which have a larger energy.

Figure 1(c) is again a second-order core polarization diagram but with a 3p-2h intermediate state. For this diagram we write

$$\begin{aligned} \delta\epsilon_j(3p-2h) &= -\frac{1}{4(2j+1)} \sum_{p,h_1,h_2,J,T} (2J+1)(2T+1) \\ &\quad \times \frac{[\langle h_1 h_2 | V | j p \rangle_{J,T}]^2}{\epsilon_{h_1} + \epsilon_{h_2} - \epsilon_j - \epsilon_p}, \end{aligned} \quad (3)$$

where the sum over the hole states h_1, h_2 is unrestricted. This expression is positive definite for the single-particle states which will be considered here. Inspecting the energy denominator again and ignoring possible differences for the matrix elements in the numerator, one would expect that this repulsion is larger for the states j with a lower energy. As a result of the combined terms (2) and (3) one therefore would expect a bunching up of the levels near the Fermi surface.

The above expressions (2) and (3) have been amply discussed by Bertsch [5] and by Bertsch and Kuo [6]. They noted that whereas the effective mass due to velocity dependence (not to be confused with the Dirac effective mass) is less than m with a bare interaction, the effect of core polarization is to cause this effective mass to be close to m near the Fermi surface. This is just another way to describe the bunching up of levels near the Fermi surface, which we have discussed above. More recently Bar-Touv and Moszkowski [7] noted that this bunching up holds for levels from different major shells, but that if one averages over the spin-orbit splitting there is no bunching up of levels of different n, l within a major shell. The work of Mahaux and Sartor [8] is also relevant concerning this point.

Numerical results in the next section will show that the 2p-1h and 3p-2h diagrams, when combined, change the single-particle energies of the spin-orbit partners $j = l - \frac{1}{2}$ and $j = l + \frac{1}{2}$ by nearly the same amount so that the single-particle splitting between $j = l - \frac{1}{2}$ and $j = l + \frac{1}{2}$ is almost unaffected.

We next consider Hartree-Fock (HF) insertions in the calculation of renormalization effects for the single-particle energies. These were not included in the work of Bertsch and Kuo [6] but they were considered in a remarkably complete work by Kassis [9] who carried out the calculations up to third order in perturbation theory. Kassis considered ${}^5\text{He}$ and ${}^{17}\text{O}$, i.e., a closed shell plus a valence nucleon. In our calculations we wish to see if the behavior for a closed shell minus one nucleon (${}^{15}\text{O}$) is similar to that of a closed shell plus a valence nucleon. Also, as mentioned before, we wish to examine the similarities and differences between the effects of the relativity and of core polarization.

We divide the HF diagrams into two classes: single HF insertions (SHF) and double HF insertions (DHF). It is convenient to define the following sum:

$$D(a, b, c, d) = \delta_{j_a, j_b} \sum_{J, T} \frac{(2J+1)(2T+1)}{2(2j_a+1)} \langle ac | V | bd \rangle_{J, T}. \quad (4)$$

In Fig. 1(d) we have the single HF insertions (SHF): V and U diagrams where U is the single-particle potential that we actually use to calculate our single-particle wave functions, i.e., the harmonic oscillator potential. The contribution from these diagrams is

$$\delta\epsilon_j(\text{SHF}) = 2 \sum_{p, h} \frac{D(j, j, p, h)}{\epsilon_h - \epsilon_p} \times \left[\sum_c D(h, p, c, c) - \langle h | U | p \rangle \right]. \quad (5)$$

For the harmonic oscillator potential $U = \frac{1}{2} m \omega^2 r^2$, we have

$$\langle h | U | p \rangle = -\frac{\hbar\omega}{2} \delta_{j_p, j_h} \delta_{l_p, l_h} \delta_{n_p, n_h+1} \times \sqrt{(n_h+1)(n_h+l_h+\frac{3}{2})}. \quad (6)$$

The minus sign comes from the convention used for the two-body matrix elements that all radial wave functions are positive near the origin. It is obvious that the particle p and hole h in Fig. 1(d) must couple to $J^\pi = 0^+$.

The contribution from the double HF insertions (DHF) [Fig. 1(e)] is

$$\delta\epsilon_j(\text{DHF}) = \sum_p \frac{\left[\sum_c D(j, p, c, c) - \langle p | U | j \rangle \right]^2}{\epsilon_j - \epsilon_p} - \sum_h \frac{\left[\sum_c D(j, h, c, c) - \langle h | U | j \rangle \right]^2}{\epsilon_h - \epsilon_j}, \quad (7)$$

where

$$\langle p | U | j \rangle = -\frac{\hbar\omega}{2} \delta_{j, j_p} \delta_{l, l_p} \delta_{n_p, n+1} \sqrt{(n+1)(n+l+\frac{3}{2})}, \quad (8)$$

$$\langle h | U | j \rangle = -\frac{\hbar\omega}{2} \delta_{j, j_h} \delta_{l, l_h} \delta_{n_h, n-1} \sqrt{n(n+l+\frac{1}{2})}. \quad (9)$$

In Eqs. (2)–(7), we approximate the single-particle energies in the energy denominators by the kinetic energy plus the one-body spin-orbit interaction:

$$\epsilon_j \simeq (2n+l+\frac{3}{2})\hbar\omega - \xi l \cdot s \quad (10)$$

with $\xi = 2$ MeV. All configurations with $2\hbar\omega$ excitations (in the case of $\xi = 0$) for the intermediate states are included. The renormalized single-particle energy for a particle in the orbit (nlj) ignoring the Hartree-Fock corrections is given by

$$\epsilon_j(R) = \epsilon_j(M) + \delta\epsilon_j(2p-1h) + \delta\epsilon_j(3p-2h), \quad (11)$$

where $\epsilon_j(M)$ refers to the mean field part given in Eq. (1) and the 2p-1h and 3p-2h corrections are defined in Eqs. (2) and (3). The total result taking into account the Hartree-Fock terms is denoted by

$$\epsilon_j(T) = \epsilon_j(R) + \delta\epsilon_j(\text{SHF}) + \delta\epsilon_j(\text{DHF}). \quad (12)$$

We now consider the renormalization of the single-hole energies. Similar to the single-particle case, the renormalized single-hole energy for a hole in the orbit (nlj) inside a core can be written as

$$\epsilon_j(R) = \epsilon_j(M) + \delta\epsilon_j(2p-3h) + \delta\epsilon_j(1p-2h), \quad (13)$$

and the contributions of the Hartree-Fock corrections can be added in the very same way as it is written in Eq. (12). Note that Eq. (13) contains the same terms as Eq. (11) except that for the case of hole states we refer to the corrections given in Eqs. (2) and (3) as (2p-3h) and (1p-2h) terms, respectively. This change of the nomenclature is made plausible from Fig. 2, where diagrams representing

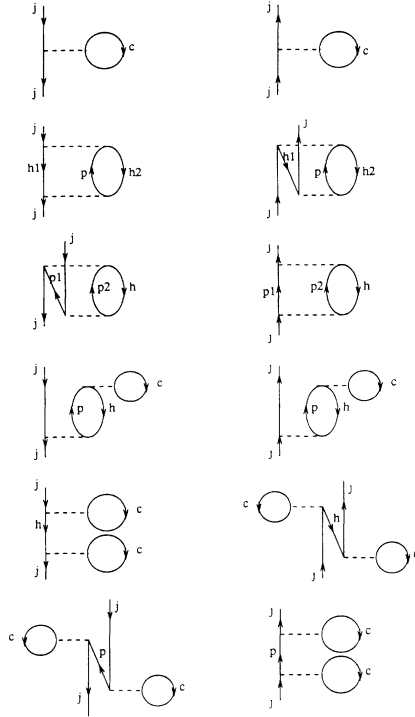


FIG. 2. Some of the first- and second-order diagrams (left) for the single-hole energies and the corresponding diagrams (right) for the single-particle energies which have the same expressions. Dashed lines represent the particle-particle interaction V .

contributions for the single-particle energies for particle and hole states are compared to each other.

For the two-body interaction employed in Eqs. (1)–(4) we consider G -matrix elements which have been determined by solving the Bethe-Goldstone equation,

$$G = \mathcal{V} + \mathcal{V} \frac{Q}{E_s - Q t Q} G, \quad (14)$$

directly in a basis of harmonic oscillator states [10]. The oscillator parameter for this basis and also for the corresponding energies in Eqs. (1), (6), (8), and (9) has been chosen to yield an oscillator energy of $\hbar\omega = 13.92$ MeV. For the starting energy [E_s in Eq. (14)], a constant value of -15 MeV has been selected and the Pauli operator Q has been defined in the oscillator basis to prevent intermediate two-particle states with one nucleon in a hole state ($0s$ and $0p$) or both nucleons in the $1s0d$ shell. In this way the particle-particle ladders of Fig. 1(b) with an excitation energy of $2\hbar\omega$ are not taken into account in the G matrix and therefore should be calculated explicitly. For the spectrum of intermediate particle states only the kinetic energy (t) is taken into account.

For the bare NN interaction \mathcal{V} we have considered various modern versions of the Bonn OBE potentials [4]. The parameters of these potentials have been adjusted to fit the NN scattering phase shifts. This has been done either by solving the Blankenbecler-Sugar equation (we will refer to these potentials, which are defined in Table A.1 of [4], as nonrelativistic interactions) or by solving the

Thompson equation. The parameters of these potentials are given in Table A.2 of [4]. These potentials have been employed in Dirac-Brueckner-Hartree-Fock calculations for ^{16}O [3]. Such calculations show that the Dirac spinors for nucleons in a nuclear medium are substantially different from the Dirac spinors of a free nucleon. The ratio of large to small components for the Dirac spinors in the medium may be described in terms of an effective mass m^* for which $m^* = 630$ MeV is a reasonable choice. Therefore we will refer to these potentials obtained from the Thompson equations as relativistic interactions and study the dependence of the resulting single-particle energies on the effective mass m^* .

For both kinds of scattering equations, Ref. [4] presents potentials with various strengths for the tensor component. We will consider in the present investigation versions A and C . While a moderate tensor force is contained in the potentials C , yielding a D -state probability for the deuteron of $P_D = 5.5\%$, the potentials A contain a rather weak tensor force ($P_D = 4.5\%$).

III. DISCUSSION OF RESULTS

As a first example we discuss the results obtained for the single-particle energies for the $p_{3/2}$ and $p_{1/2}$ hole states in ^{16}O which are given in Table I. The first column shows the results obtained in the mean field approximation [$\epsilon(M)$, defined in Eq. (1)]. Considering the nonrelativistic approaches (NRBA and NRBC), the energies for the $p_{3/2}$ state are -25.17 and -23.84 MeV for versions A and C , respectively. Therefore the binding energy is a bit larger than the experimental value of -21.8 MeV, which is derived from the energy difference between the ground states of ^{16}O and ^{15}O .

The agreement for the single-particle energy could be improved by a self-consistent choice for the starting energy E_s in the Bethe-Goldstone equation (14). The value chosen for all the results which we present here is $E_s = -15$ MeV, which is quite appropriate for the mean field term of the d states [note that a self-consistent choice in Eq. (1) would require $E_s = \epsilon_j + \epsilon_c$]. For the states in the p shell a more negative starting energy should be chosen. If we use $E_s = -30$ MeV, the single-particle energies would be less attractive by around 1 MeV. Since, however, all other quantities listed in Table I, like the effects of the core polarization terms or the results for the spin-orbit splittings, are hardly affected by the choice of the starting energy, we have chosen to present results for a fixed value of E_s .

Comparing different versions for the NN interaction, we see that the interactions with a weaker tensor force (A) yield more attractive single-particle energies than those with a stronger tensor force (C). This is the same feature as observed in the BHF calculations. Comparing the saturation points of nuclear matter (and also finite nuclei) obtained for various realistic NN interactions, one finds that these results form a ‘‘Coester’’ band [11], such that interactions with a weaker tensor force lead to more binding energy than those with a stronger tensor force, as the Pauli effects in the Bethe-Goldstone equation reduce the attraction in the G matrix more in the latter than in

TABLE I. Single-particle energies for the $p_{3/2}$ and $p_{1/2}$ hole states in ^{16}O are presented as obtained in the mean field approximation [$\epsilon(M)$, see Eq. (1)], with inclusion of core polarization corrections from 1p-2h, 2p-3h diagrams [$\epsilon(R)$, see Eq. (13)], and adding the Hartree-Fock corrections [$\epsilon(T)$, see Eq. (12)]. Also, the sums of the individual contributions are given. Nonrelativistic Bonn A (NRBA) and Bonn C (NRBC) and relativistic Bonn A (RBA) and Bonn C (RBC) interactions with different values of Dirac effective nucleon mass m^* are used. All energies are in units of MeV. Also given is the spin-orbit splitting $\Delta\epsilon = \epsilon_{p_{1/2}} - \epsilon_{p_{3/2}}$. The experimental data to compare to are -21.8 MeV for the single-particle energy of the $p_{3/2}$ state and 6.176 MeV for the spin-orbit splitting $\Delta\epsilon$.

Interaction	Orbit	$\epsilon(M)$	$\delta\epsilon(1p-2h)$	$\delta\epsilon(2p-3h)$	$\epsilon(R)$	$\delta\epsilon(\text{SHF})$	$\delta\epsilon(\text{DHF})$	$\epsilon(T)$
NRBA	$p_{3/2}$	-25.17	4.50	-4.87	-25.54	-5.30	-1.20	-32.03
	$p_{1/2}$	-21.00	5.03	-5.39	-21.36	-3.04	-0.83	-25.23
	$\Delta\epsilon$	4.17	0.53	-0.52	4.18	2.25	0.37	6.80
RBA $m^*/m=1$	$p_{3/2}$	-23.25	3.62	-3.82	-23.46	-3.87	-0.70	-28.04
	$p_{1/2}$	-19.31	4.19	-4.24	-19.36	-2.18	-0.44	-21.98
	$\Delta\epsilon$	3.95	0.57	-0.41	4.11	1.69	0.26	6.06
RBA $m^*/m=0.78$	$p_{3/2}$	-21.54	3.42	-3.52	-21.64	-2.14	-0.29	-24.07
	$p_{1/2}$	-16.29	3.98	-4.00	-16.31	-0.73	-0.09	-17.14
	$\Delta\epsilon$	5.24	0.56	-0.48	5.33	1.41	0.19	6.92
RBA $m^*/m=0.67$	$p_{3/2}$	-20.21	3.29	-3.32	-20.24	-1.04	-0.10	-21.38
	$p_{1/2}$	-14.05	3.87	-3.88	-14.05	-0.11	0.00	-14.16
	$\Delta\epsilon$	6.16	0.59	-0.56	6.19	0.93	0.10	7.22
NRBC	$p_{3/2}$	-23.84	4.26	-4.65	-24.24	-4.38	-0.89	-29.51
	$p_{1/2}$	-19.69	4.84	-5.22	-20.07	-2.42	-0.58	-23.07
	$\Delta\epsilon$	4.15	0.59	-0.57	4.16	1.97	0.31	6.44
RBC $m^*/m=1$	$p_{3/2}$	-20.99	3.34	-3.60	-21.26	-2.53	-0.35	-24.14
	$p_{1/2}$	-17.09	3.97	-4.07	-17.19	-1.32	-0.18	-18.68
	$\Delta\epsilon$	3.91	0.63	-0.47	4.07	1.21	0.17	5.46
RBC $m^*/m=0.78$	$p_{3/2}$	-19.15	3.14	-3.31	-19.32	-1.00	-0.08	-20.40
	$p_{1/2}$	-13.95	3.77	-3.85	-14.03	-0.23	0.00	-14.26
	$\Delta\epsilon$	5.20	0.63	-0.54	5.29	0.77	0.08	6.13
RBC $m^*/m=0.67$	$p_{3/2}$	-17.71	3.01	-3.12	-17.83	-0.04	0.00	-17.87
	$p_{1/2}$	-11.60	3.66	-3.74	-11.68	0.13	-0.04	-11.59
	$\Delta\epsilon$	6.11	0.65	-0.61	6.15	0.18	-0.04	6.28

the former case [3,4,12].

It is furthermore remarkable that the results obtained for the relativistic cases (RBA and RBC, Thompson equation, $m^*=m$) are less attractive than those for the nonrelativistic approaches. The same feature can also be observed in BHF calculations for finite nuclei [3,12] while in nuclear matter the relativistic potentials yield more binding energy (for $m^*=m$) than the calculations employing the Blankenbecler-Sugar equation [4]. This could be a consequence of the fact that the Blankenbecler-Sugar potentials are fitted with an attraction of shorter range in the channels with isospin $T=1$, as the mass of the σ meson has been chosen to be larger for these channels.

While single-particle energies depend on the choice of the interaction, the spin-orbit splitting is almost not affected, as long as we do not consider any change of the Dirac spinors, i.e., we keep $m^*=m$. This splitting is 4.2 MeV in the case of the nonrelativistic choice and 3.9 MeV for the relativistic cases, almost independent on the strength of the tensor force. These values are too small compared to the experimental splitting, which is 6.176 MeV. If, however, we consider a change of the Dirac spinors in the nuclear medium by decreasing the effective mass we find that the spin-orbit splitting is enhanced considerably. This is the relativistic effect that we have already discussed in the section describing the motivation

for this investigation (see also [13,14]). Using an effective mass $m^*=630$ MeV ($m^*/m=0.67$), which is supported by DBHF calculations for nucleons occupying levels inside the nucleus [3], we obtain values for the spin-orbit splitting of 6.16 MeV (A) and 6.11 MeV (C), which are in good agreement with the experimental data, again nearly independent on the strength of the tensor force considered.

Furthermore, one finds that the reduction of the effective mass decreases the absolute value of the single-particle energy. This is of course a consequence of the well-known relativistic effect that the attractive components of the NN interaction in the medium are reduced if the Dirac spinors of the nucleons are modified in a self-consistent way [3,15].

We are now going to discuss the effects of the core polarization terms displayed in Figs. 1(b) and 1(c) and evaluated as given in Eqs. (2) and (3). Note that the hole states h , h_1 , and h_2 appearing in these equations are summed over all core orbits; the particle states p , p_1 , and p_2 take all possible orbits outside the core with the restriction that the energy denominator be equal to $-2\hbar\omega$ in the absence of the spin-orbit interaction [$\xi=0$ in Eq. (10)].

As we have already discussed in Sec. II, the 1p-2h contribution turns out to yield a repulsive contribution to the single-particle energies for the p states. From an inspec-

tion of the energy denominators in Eq. (3) alone, one could have expected the correction to be larger for the $p_{3/2}$ state than for the $p_{1/2}$ state. The calculations show, however, that the opposite is true because of the different matrix elements in the numerator of Eq. (3). Therefore the 1p-2h contributions enhance the spin-orbit splitting by a value typically of 0.53–0.65 MeV, depending on which model is used for the NN interaction.

As we expected from our discussion of Eq. (2), the 2p-3h corrections to the single-particle energies turn out to be attractive. Also in this case the effects are larger for the $p_{3/2}$ state compared to the $p_{1/2}$ state due to differences in the matrix elements in Eq. (2). Therefore the 2p-3h terms reduce the spin-orbit splitting. We observe a remarkable cancellation between the 2p-3h and 1p-2h correction terms. While each core polarization term alone leads to modifications for the single-particle energies and the spin-orbit splittings up to 20%, the total effect of these corrections is negligible. This cancellation is an observation supporting our double partitioning for the treatment of correlations. Note that the effects of particle-particle ladders with intermediate states of energies above $2\hbar\omega$ have been considered by solving the Bethe-Goldstone equation, while the effects of particle-particle terms at low energies have been combined with those of intermediate hole-hole states in our explicit perturbative calculation, evaluating diagrams of Figs. 1(b) and 1(c), which leads to the cancellation we have just discussed. Therefore the inclusion of core polarization

terms does not destroy the good agreement obtained for the spin-orbit splitting already in the mean field approximation, if the change of the Dirac spinors is taken into account.

It should be mentioned that BHF and also DBHF calculations try to include particle-particle terms at all energies but ignore the effects of hole-hole scattering terms. This is justified for the excitations at high energies, as there are no hole-hole excitations at such high energies. For the low-energy excitations it might be preferable to include particle-particle terms and hole-hole terms in a symmetric way [8,16]. Our investigations also show that the single-particle energies obtained in BHF calculations should be modified according to the corrections listed in the second column of Tables I and II.

Finally, we consider the corrections due to the Hartree-Fock insertions displayed in Figs. 1(d) and 1(e). These terms represent a perturbative approach to evaluate the diagrams of Figs. 1(a)–1(c), in particular, the mean field diagram of Fig. 1(a) in terms of self-consistent BHF single-particle states rather than using the basis of harmonic oscillator states. Since the expansion nucleon self-energy should converge better in a self-consistent basis, it is of course conceptually favorable to include the Hartree-Fock terms. However, one has to be aware that self-consistent BHF or DBHF calculations employing the OBE potentials that we also use in our present investigations tend to produce single-particle wave functions, which lead to a radius for ^{16}O , much smaller than the ex-

TABLE II. Single-particle energies for the $d_{5/2}$ and $d_{3/2}$ particle states in ^{16}O . The experimental data to compare to are -4.14 MeV for the single-particle energy of the $d_{5/2}$ state and 5.086 MeV for the spin-orbit splitting $\Delta\epsilon$. See Table I for further information.

Interaction	Orbit	$\epsilon(M)$	$\delta\epsilon(3p-2h)$	$\delta\epsilon(2p-1h)$	$\epsilon(R)$	$\delta\epsilon(\text{SHF})$	$\delta\epsilon(\text{DHF})$	$\epsilon(T)$
NRBA	$d_{5/2}$	-4.61	2.00	-3.55	-6.15	-1.26	-0.12	-7.53
	$d_{3/2}$	1.53	2.64	-4.63	-0.46	0.91	-0.05	0.40
	$\Delta\epsilon$	6.14	0.64	-1.09	5.69	2.18	0.07	7.93
RBA $m^*/m=1$	$d_{5/2}$	-3.42	1.54	-2.77	-4.65	-1.05	-0.01	-5.71
	$d_{3/2}$	2.38	2.18	-3.71	0.85	0.56	-0.17	1.24
	$\Delta\epsilon$	5.80	0.64	-0.95	5.50	1.61	-0.15	6.95
RBA $m^*/m=0.78$	$d_{5/2}$	-1.94	1.41	-2.57	-3.09	-0.47	-0.02	-3.59
	$d_{3/2}$	5.58	2.04	-3.57	4.05	0.83	-0.67	4.22
	$\Delta\epsilon$	7.52	0.62	-1.00	7.14	1.31	-0.65	7.80
RBA $m^*/m=0.67$	$d_{5/2}$	-0.81	1.33	-2.44	-1.92	-0.14	-0.11	-2.18
	$d_{3/2}$	7.91	1.96	-3.53	6.34	0.71	-1.23	5.82
	$\Delta\epsilon$	8.72	0.62	-1.09	8.26	0.86	-1.12	7.99
NRBC	$d_{5/2}$	-3.58	1.84	-3.30	-5.04	-1.03	-0.04	-6.11
	$d_{3/2}$	2.52	2.60	-4.42	0.69	0.85	-0.13	1.41
	$\Delta\epsilon$	6.10	0.76	-1.12	5.74	1.88	-0.10	7.52
RBC $m^*/m=1$	$d_{5/2}$	-1.65	1.37	-2.51	-2.80	-0.64	-0.01	-3.44
	$d_{3/2}$	4.09	2.12	-3.52	2.68	0.51	-0.40	2.79
	$\Delta\epsilon$	5.74	0.75	-1.01	5.48	1.15	-0.39	6.24
RBC $m^*/m=0.78$	$d_{5/2}$	-0.11	1.25	-2.33	-1.19	-0.16	-0.14	-1.49
	$d_{3/2}$	7.33	1.98	-3.38	5.93	0.55	-1.09	5.39
	$\Delta\epsilon$	7.45	0.73	-1.06	7.12	0.71	-0.95	6.88
RBC $m^*/m=0.67$	$d_{5/2}$	1.06	1.18	-2.20	0.03	0.11	-0.33	-0.19
	$d_{3/2}$	9.71	1.90	-3.35	8.26	0.26	-1.80	6.72
	$\Delta\epsilon$	8.65	0.72	-1.14	8.23	0.15	-1.47	6.91

perimental value [3,12]. Therefore it may be favorable to ignore the Hartree-Fock corrections and stick to the original oscillator wave functions since they yield much more realistic radii.

This dilemma has also been observed, e.g., by Hjorth-Jensen *et al.* [17]. In evaluating the renormalization of the effective two-body interaction to be used in *sd*-shell model calculations, they find that the choice of self-consistent BHF wave functions improves the convergence of the expansion. On the other hand, however, the resulting matrix elements obtained in the BHF basis are much less realistic than those obtained in an appropriate oscillator basis. Hjorth-Jensen *et al.* relate this deficiency of the results in the BHF basis to the fact that the BHF wave functions are localized too much to the center of the nucleus.

Because of this experience we prefer to evaluate in a first step the single-particle energies and the spin-orbit splitting in an oscillator basis, using wave functions with realistic radii, as we have discussed up to now. In a second step we can now determine the modifications which are due to the Hartree-Fock self-consistency and discuss those effects separately.

Inspecting the effects of the HF correction terms presented in Table I, one observes quite a substantial increase in the binding energies for the single-particle states. The size of the effect is directly related to the change of the radius obtained in the BHF calculation as compared to the oscillator model: The potentials with weak tensor force (*A*) tend to give smaller radii than those with a stronger tensor component (*C*) [12] and also the Hartree-Fock corrections listed in Table I are larger for the former as compared to the latter cases. Relativistic potentials yield larger radii than those from nonrelativistic treatment, in particular, if $m^* < m$, and therefore the energy corrections are smaller in the former case. Anyway, with inclusion of the Hartree-Fock corrections the single-particle states are too much bound as compared to the empirical values, in particular, if the relativistic effects are ignored. Also, the results for the spin-orbit splitting tend to be too large.

Results for the single-particle energies of the $d_{5/2}$ and $d_{3/2}$ particle states and the corresponding spin-orbit splitting are listed in Table II. Many features are identical to those discussed for the *p* states. Therefore we will concentrate the discussion on differences between the two cases. The mean field predictions $\epsilon(M)$ for the $d_{5/2}$ state are in reasonable agreement with the experimental data. The nonrelativistic interaction *A* yields slightly too much binding, whereas the nonrelativistic potential *C* and both relativistic treatments (*A* and *C*) give too little binding for the $d_{5/2}$ state. This is particularly true for those cases for which we consider an effective Dirac mass m^* smaller than the bare mass. In this case, however, one must keep in mind that a nucleon moving at the surface of ^{16}O in a $d_{5/2}$ orbit is exposed to an average nuclear density which is much smaller than the typical density for nucleons occupying states of the core. Therefore it seems to be more realistic to consider an effective mass m^* which is close to the bare mass or even identical to the bare mass.

If now we compare the mean field predictions for spin-

orbit splitting in the *p*-shell and in the *d*-shell case by case, we find that the splitting obtained for the *d* shell is always larger than that for the *p* shell. This is the behavior one would expect from a simple one-body spin-orbit interaction of the form $-\xi \mathbf{l} \cdot \mathbf{s}$, as we discussed in the Introduction. If, however, we now take into account relativistic effects and, following the arguments outlined just before, use $m^*/m = 0.67$ for the *p* shell and $m^* = m$ for the *d* shell, we find that this yields a spin-orbit splitting, which is slightly larger in the *p* shell (6.1 MeV) than in the *d* shell (5.8 MeV). This result is almost independent on the potential that is used (*A* or *C*) and shows the same tendency as experiment (6.2 MeV for *p* shell and 5.1 MeV for *d* shell).

That the effects of the core polarization terms are smaller for the *d* states may indicate that the typical matrix elements occurring in the numerators of Eqs. (2) and (3) are smaller than those for the *p* states. The cancellation between 3*p*-2*h* and 2*p*-1*h* is not as complete as it is in the case of corresponding terms in the *p* shell. For the states above the Fermi surface the particle-particle ladder term of Fig. 1(b) is enhanced as compared to the hole-hole term, which can be understood from the energy denominators discussed in Sec. II. Therefore the combined core polarization terms slightly enhance the attraction for the single-particle energies, which for most cases improve the agreement with experiment, and decrease the spin-orbit splitting. For the example that, according to the earlier discussion, is our most favorable one for the *d* shell, the relativistic case $m^* = m$, this yields a reduction from 5.8 to 5.5 MeV.

Finally, we mention that the effects of the Hartree-Fock correction terms are smaller than in the case of the *p* shell. This can be interpreted as an indication that the BHF wave functions for the particle states are less localized than those for the hole states. Therefore the BHF wave functions for the *d* state are closer to the oscillator approach and the correction gets smaller. For the spin-orbit splitting we observe some cancellations between the SHF and DHF terms, while their combination enhances the spin-orbit splitting coherently. One may argue that this demonstrates that, employing self-consistent wave functions, the spin-orbit splittings for the particle states tend to be reduced as compared to those for the hole states since the particle states are less localized. At the present stage, however, this conclusion must be considered with some care as the BHF wave functions for modern OBE potentials yield nuclear radii, which are too small compared with experiment (see discussion above).

IV. ADDITIONAL REMARKS AND CONCLUSION

It is the main purpose of the present investigation to compare the spin-orbit splitting for the single-particle shells just above and below the Fermi level. As an example we consider ^{16}O , for which the experimental data show a larger spin-orbit splitting for the *p* shell (6.176 MeV) than for the *d* shell (5.086 MeV). This is contrary to the predictions of a simple $-\xi \mathbf{l} \cdot \mathbf{s}$ term which yields a larger splitting for the larger orbital angular momentum and also to the predictions of Hartree-Fock calculations

using phenomenological forces [1] or realistic forces (see discussion in the preceding section) which yield spin-orbit splittings increasing with l .

We observe the following mechanisms to reduce the spin-orbit splittings of the particle shells as compared to the hole shells.

(i) The change of the Dirac spinors in the nuclear medium obtained in Dirac-Brueckner-Hartree-Fock (DBHF) calculations can be described in terms of an effective Dirac mass m^* which is much smaller in the interior of the nucleus than at the surface. Since the spin-orbit splitting is to first order proportional to the inverse of m^* [13,14], this enhances the spin-orbit splittings for the hole states as compared to those of the particle states.

(ii) The core polarization effects due to low-energy excitations in the intermediate states of Figs. 1(b) and 1(c) tend to cancel each other. This cancellation is almost complete for the p states in ^{16}O . For the particle states (d) the particle-particle ladder term of Fig. 1(b) gets more important as compared to the hole-hole term in Fig. 1(c), which reduces the spin-orbit splitting slightly. Both of these effects are clearly established in our investigation.

(iii) Self-consistent wave functions for the particle states are less localized than those of hole states, even beyond effects contained in an oscillator model. This tends to reduce the spin-orbit splitting of the particle states as compared to those in hole shells. Unfortunately, the OBE potentials employed in the present investigation produce BHF wave functions with a radius too small as compared to experiment [3,12]. Therefore the BHF

corrections may not be very realistic and must be considered with some care.

Approximating the single-particle wave functions by harmonic oscillator waves with realistic radii, we obtain results in good agreement with the experimental data not only for the spin-orbit splittings but also for the single-particle energies for the particle and hole states. Considering the relativistic potential A of [4] and taking into account the change of the Dirac spinors as a function of density, we obtain -20.24 and -4.65 MeV for the energy of the $p_{3/2}$ and $d_{5/2}$ states, respectively, which is in good agreement with the experimental data: -21.8 and -4.1 MeV. Also the results obtained for the spin-orbit splitting (6.19 MeV for p and 5.50 MeV for d shell) are in fair agreement with the data.

A problem, which remains to be solved, is to find out why microscopic many-body calculations using modern OBE potentials fail to predict the correct radius. Only after the solution of this problem reliable calculations can be performed which account for the effects of single-particle wave functions which are determined in a self-consistent way.

This work was supported by the U.S. Department of Energy under Grant No. DE-FG05-86ER-40299, by NSERC Canada under operating Grant No. A-3198, and by the Deutsche Forschungsgemeinschaft (DFG Fa 67/14-1). We thank Paul Ellis for a useful discussion. We also thank Donald Sprung for reading the manuscript and for his interest.

-
- [1] M. Beiner, H. Flocard, and Nguyen van Giai, Nucl. Phys. **A238**, 29 (1975).
 [2] D. C. Zheng, L. Zamick, and H. Müther, Phys. Rev. C **45**, 275 (1992).
 [3] H. Müther, R. Machleidt, and R. Brockmann, Phys. Rev. C **42**, 1981 (1990).
 [4] R. Machleidt, Adv. Nucl. Phys. **19**, 189 (1989).
 [5] G. F. Bertsch, Nucl. Phys. **74**, 234 (1965).
 [6] G. F. Bertsch and T. T. S. Kuo, Nucl. Phys. **A112**, 204 (1968).
 [7] J. Bar-Touv and S. A. Moszkowski, Phys. Lett. B **244**, 143 (1990).
 [8] C. Mahaux and R. Sartor, Nucl. Phys. **A475**, 247 (1987).
 [9] N. I. Kassis, Nucl. Phys. **A194**, 205 (1972).
 [10] H. Müther and P. U. Sauer, in Computational Methods in Nuclear Physics (Springer, in press), Vol. II.
 [11] F. Coester, S. Cohen, B. D. Day, and C. M. Vincent, Phys. Rev. C **1**, 769 (1970).
 [12] K. W. Schmid, H. Müther, and R. Machleidt, Nucl. Phys. **A530**, 14 (1991).
 [13] G. E. Brown, H. Müther, and M. Prakash, Nucl. Phys. **A506**, 565 (1990).
 [14] R. Brockmann and W. Weise, Phys. Rev. C **16**, 1282 (1977).
 [15] B. D. Serot and J. D. Walecka, Adv. Nucl. Phys. **16**, 1 (1986).
 [16] M. Borromeo, D. Bonatsos, H. Müther, and A. Polls, Nucl. Phys. **A539**, 189 (1992).
 [17] M. Hjorth-Jensen, E. Osnes, H. Müther, and K. W. Schmid, Phys. Lett. B **248**, 243 (1990); M. Hjorth-Jensen, E. Osnes, and H. Müther, Ann. Phys. **213**, 102 (1992).